

Short Communication

Solid-State Characterization of Buspirone Hydrochloride Polymorphs

M. Sheikhzadeh,¹ S. Rohani,^{1,3} A. Jutan,¹ T. Manifar,¹ K. Murthy,² and S. Horne²

Received August 29, 2005; accepted December 21, 2005

Abstract. The purpose of this study was to characterize Form 1 and Form 2 of buspirone hydrochloride, an anxiolytic medicine. The techniques used for characterization included microscopy (optical, hot stage, and scanning electron microscopy), thermal analysis (differential scanning calorimetry and thermogravimetric analysis), solid-state Fourier transform infrared (FTIR) spectroscopy, X-ray powder diffractometry (XRPD), and Raman spectroscopy. Morphologically, Form 1 and Form 2 consist of plate and columnar crystals, respectively, with good filterability. Thermal analysis showed that the two forms are enantiotropic over the studied temperature range. The FTIR method was used successfully for the quantification of Form 1 in a mixture of Forms 1 and 2. The ratio of a characteristic peak to a reference peak and the chemometric method were used to obtain the calibration curve. The Raman peak shifts showed the difference between the two forms especially for the n-butyl group. The large number of distinguishable XRPD peaks in the region of 5° to 30° 2θ of the two polymorphs demonstrated that XRPD is a useful tool for quantitative and qualitative analysis of polymorphs.

KEY WORDS: buspirone hydrochloride; characterization; polymorphism.

INTRODUCTION

Polymorphism has been recognized as an important element of drug development. Many pharmaceutical solids can exist in different polymorphic forms. The polymorphs differ in internal solid-state structure and possess different physical properties, such as stability, dissolution rate, and bioavailability, which may affect drug processability and quality/performance. Differences in the physical, chemical, and mechanical properties of the active pharmaceutical ingredient (API) should be clearly described in filing of new drug applications (NDAs) and abbreviated new drug applications (ANDAs) (1). Pharmaceutical manufacturers often select a special form that has the desirable characteristics.

Buspirone hydrochloride is an anxiolytic drug. The mechanism by which buspirone works is not fully understood; it seems to act by modifying the release of a mixture of neurotransmitters in the brain. Neurotransmitters are chemicals that are stored in nerve cells and are involved in transmitting messages between the nerve cells.

Buspirone hydrochloride is a white, crystalline, water-soluble compound with a molecular mass of 422. Chemically, buspirone hydrochloride (BUS-HCl) is *N*-[4-[4-(2-pyrimidinyl)-1-piperazinyl] butyl]-1,1-cyclopentanediacetamide monohydrochloride. The molecular formula C₂₁H₃₁N₅O₂·HCl is represented by the structural formula shown in Scheme 1. It has been discovered that solid BUS-HCl can exist in two different polymorphic forms (2).

A number of methods are currently employed for characterizing pharmaceutical solid polymorphs (9). X-ray powder diffraction (XRPD) identifies the polymorphs as a result of the differences in unit cell dimensions. Fourier transform infrared (FTIR) and Raman spectroscopy methods are based on the detection of properties that are associated with molecular level. The melting point of Form 1 was reported as 188°C and that of Form 2 is in the range 202–204°C (2). Chilmonczyk *et al.* (3) have reported the NMR spectroscopy of solid BUS-HCl without mentioning the polymorphic form. Based on their research, the theoretical calculations suggest that the NH⁺ band in BUS-HCl reflects the formation of a moderately strong hydrogen bond between the protonated piperazine nitrogen atom (bound to the butyl spacer) and chlorine anion.

In this study, characterization of BUS-HCl by thermal analysis, Raman and FTIR spectroscopy, and XRPD has been carried out.

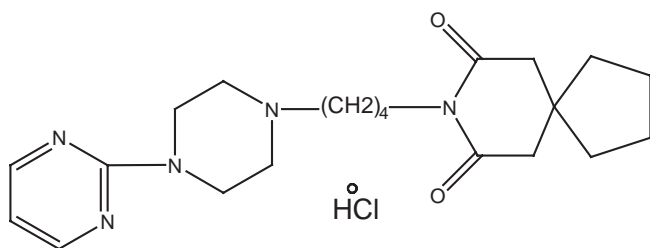
MATERIALS AND METHODS

Buspirone base was supplied by Apotex PharmaChem Inc. (Brantford, ON, Canada). Other chemicals were purchased from Caledon (Georgetown, ON, Canada) and EMD (Gibbstown, NJ, USA).

¹Department of Chemical and Biochemical Engineering, The University of Western Ontario, London, Ontario, N6A 5B9, Canada.

²Apotex PharmaChem Inc., Brantford, Ontario, N3T 5W5, Canada.

³To whom correspondence should be addressed. (e-mail: srohani@uwo.ca)



Scheme 1. Chemical structure of BUS-HCl.

Recrystallization of Buspirone Base

Buspirone base was purified using isopropanol (IPA, 99.5%) as solvent. Water-damped buspirone base was dissolved in IPA and heated to 68–72°C. The hot solution was filtered and washed with hot IPA. Then the solution was concentrated by evaporation. The concentrated solution was cooled to 0–5°C at a cooling rate of 1°C/min and maintained at that temperature for 3 h. The product was filtered, washed, with cold IPA, and dried under vacuum to obtain pure buspirone base.

Preparation of BUS-HCl Form 2

BUS-HCl Form 2 was produced by the reaction between buspirone base and HCl. After complete dissolution of buspirone base in IPA at 45–50°C, the pH of the solution was adjusted to 3.4 to 3.6 by slow addition of hydrochloric acid (38%). During the pH adjustment, temperature was maintained at 45–50°C. The solution was cooled to 20–25°C at a

cooling rate of 1°C/min under nitrogen and maintained at that temperature for 2–3 h. The product (BUS-HCl Form 2) was filtered, washed with IPA, and dried at 30–35°C under vacuum. The polymorphic identity of the final product was confirmed by DSC and FTIR analysis.

Preparation of BUS-HCl Form 1

BUS-HCl Form 1 was produced by conversion of Form 2 (2). A suspension of Form 2 in IPA was heated at 40–42°C for 20 h. The suspension was cooled at a cooling rate of 1°C/min to ambient temperature and the solids collected on a filter, washed with IPA, and dried under vacuum. The polymorphic identity of the final product was confirmed by DSC and FTIR analysis.

Optical and Scanning Electron Microscopy

An optical microscope (ZEISS, North York, ON, Canada) with a magnification of $\times 50$ to $\times 500$, equipped with a digital camera and Northern Eclipse v6.0 imaging software, was used for visual analysis. A scanning electron microscope (SEM) was used for morphological analysis (Hitachi S-4500, Tokyo, Japan). The samples were gold-sputtered.

Thermal Analysis

Hot-Stage Microscopy (HSM)

Thermal transitions in the samples were studied using a Lincam LTS 350 hot stage (Surrey, UK) and a ZEISS micro-

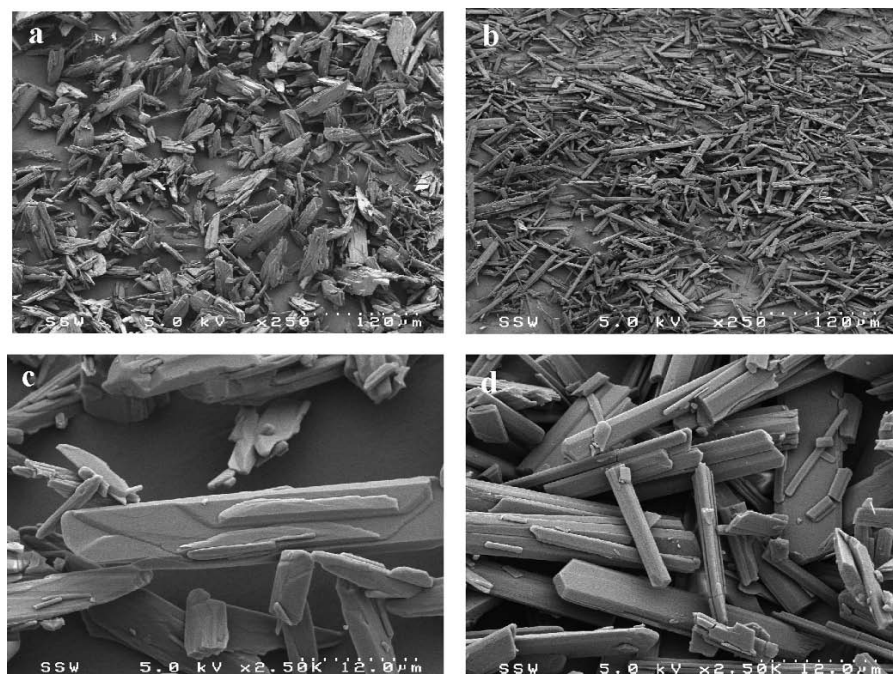


Fig. 1. Particle morphology of BUS polymorphs: (a, c) Form 1, (b, d) Form 2.

Table I. Melting Point and Heat of Melting of BUS-HCl Polymorphs

Polymorph	T_{melt} (°K)	ΔH_{melt} (kJ/mol)	$\Delta H_{\text{recrystallization}}$ (kJ/mol)
Form 1	462.95	47.219	0.151
Form 2	476.75	42.16	–

scope. The samples were heated by a Lincom TNS 594 programmable heater.

Differential Scanning Calorimetry (DSC)

Thermal analysis was done using a Mettler Toledo 822° differential scanning calorimeter (Greifensee, Switzerland) operating with version 6.1 Star° software. The samples (4–15 mg) were prepared in a covered aluminum crucible having pierced lids to allow escape of volatiles. Heating rates of 1, 5, 10, 20, 50, and 100°C/min were employed. The sensors and samples were under nitrogen purge during the experiments.

Thermogravimetric analysis (TGA)

Mass losses of the samples as a function of temperature were determined using Mettler Toledo 851° TGA system operating with version 6.1 Star° software. The sample preparation was the same as with the DSC. A heating rate of 10°C/min was employed.

Fourier Transform Infrared Spectroscopy

Qualitative Analysis

FTIR spectra were recorded on a solid-state Fourier transformation infrared spectrometer (Bruker Vector 22, Billerica, MA, USA) equipped with OPUS v3.1. The samples were analyzed by FTIR in transmission mode through a diamond window. The number of scans was 32 over the 450–4000 cm^{-1} spectral region with a resolution of 2 cm^{-1} . The background was collected in the same range for air.

Quantitative Analysis

The peak at 1153 cm^{-1} was considered for quantitative analysis of polymorphic forms. Because of possible polymorphic transformation, grinding was avoided. Spectra of pure Form 1 and 2 and known mixtures of Form 1 in Form 2 were analyzed in triplicate and the average was chosen for analysis. The spectrum for each sample was recorded over the 450–4000 cm^{-1} spectral region with 2 cm^{-1} resolution. To improve the results, the ratio of the height of the characteristic peak to an inert peak was used. The peak at 1193 cm^{-1} was considered as the inert peak. Principal component regression (PCR) and partial least squares (PLS) methods were applied for calibration of mixtures of two polymorphs (4).

X-Ray Powder Diffraction

XRPD spectra were collected on a Rigaku-Geigerflex CN2029 powder diffractometer (Tokyo, Japan), using CuK_α (λ for $\text{K}_\alpha = 1.54184 \text{ \AA}$) radiation obtained at 40 kV and 35 mA. The scans were run from 5.0° to 95.0° 2θ , increasing at a step size of 0.05° with accounting time of 2 s for each step.

Laser Raman Spectroscopy

The Raman experiment was done on a Renishaw Raman spectrometer Model 2000 (Gloucestershire, UK) using a 50× objective full power, approximately 2 mW and 633-nm laser.

RESULTS AND DISCUSSION

Morphology

Figure 1 shows the crystal shape of BUS-HCl polymorphic forms at two magnifications ($\times 250$ and $\times 2500$). SEM micrographs show that Form 1 has irregular platelike crystals with average size of $17 \times 4 \times 45 \text{ }\mu\text{m}$. Form 2 consists of regular columnar crystals with average size of $16 \times 3 \times 92 \text{ }\mu\text{m}$ and lower degree of agglomeration than Form 1.

Thermal Analysis

DSC of Form 1 at a heating rate of 1°C/min showed a phase transformation to a more stable phase. Form 1 exhibited one endotherm at 189°C (the melting point of Form 1), an exotherm at 192°C for crystallization to Form 2, and another endotherm at 203°C for melting of the recrystallized Form 2. At a heating rate of 10°C/min, the recrystallization peak and melting of Form 2 peak were lower

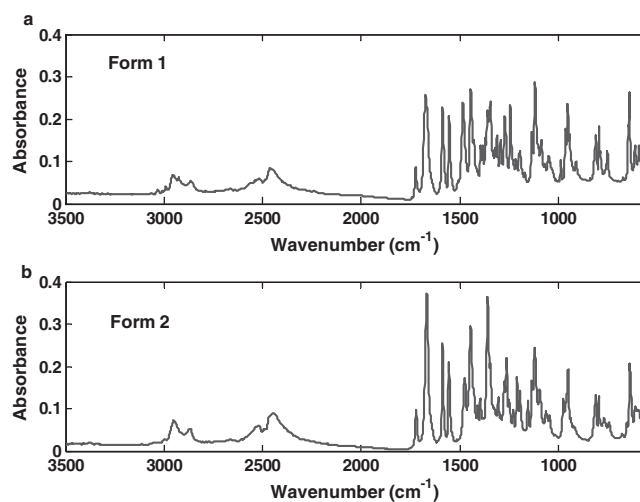


Fig. 2. The entire FTIR spectra of BUS-HCl polymorphs: (a) Form 1, (b) Form 2.

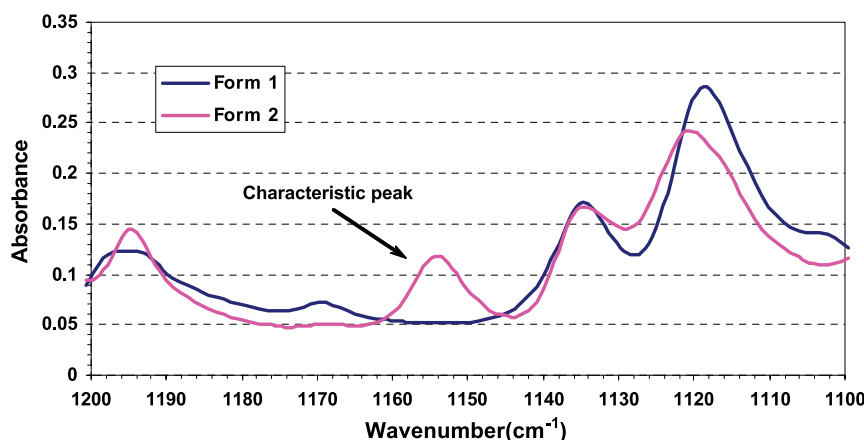


Fig. 3. The FTIR spectra and characteristic peaks over the range 1100 to 1200 cm^{-1} .

compared to the heating rate of $1^\circ\text{C}/\text{min}$. As the heating rate was increased to $50^\circ\text{C}/\text{min}$, there was a wide peak with onset at 189°C . To calculate heats of melting of Form 1, the DSC spectrum of Form 1 with heating rate of $10^\circ\text{C}/\text{min}$ was considered. The heat of recrystallization of Form 2 was very small. Form 2 yielded a single melting point at 203°C , and changing the heating rate did not have any effect on the thermogram. An optical microscope equipped with a hot stage (HSM) also confirmed the melting point temperature and transformation of the two forms.

Table I presents the measured values of melting temperature and the calculated heat of melting for both polymorphic forms of BUS-HCl. According to the Burger and Ramberger polymorphic rules (5,6), the two forms are enantiotropically related, because $T_{\text{melt } 1} < T_{\text{melt } 2}$ and $\Delta H_{\text{melt } 1} > \Delta H_{\text{melt } 2}$. In addition, it is generally accepted that for the enantiotropic forms, the solid–solid transition occurs when the two forms are conformationally related or the molecular arrangement in the crystal is close.

No mass losses were observed during TGA analysis of either forms, indicating that the forms were anhydrous and nonsolvated.

Solid-State FTIR

Solid-state FTIR spectroscopy can be used for both quantitative and qualitative analysis of drugs (8).

Qualitative Analysis

The key factor for qualitative analysis of polymorphs is finding the characteristic wavelength of each form. Figure 2 shows the FTIR spectra of BUS-HCl polymorphs. Both forms indicate a strong absorbance band due to C=O stretching vibrations in the region $1650\text{--}1700\text{ cm}^{-1}$. Both forms also indicate a strong absorbance band due to C=C stretching vibrations in the region $1600\text{--}1500\text{ cm}^{-1}$ and a broad absorbance band in the region $3000\text{--}3100\text{ cm}^{-1}$ due to C–H in aromatic rings. The band associated with C–N stretching appears in the region $1130\text{--}1270\text{ cm}^{-1}$ in Form 2, with a small shoulder. The band due to C–H scissoring and

bending vibration is present at 1380 cm^{-1} , with a larger absorbance for Form 2. Form 2 exhibits a unique absorption band at 1153 cm^{-1} . This band is very useful for qualitative and quantitative determination of BUS-HCl polymorphs.

Quantitative Analysis

In the case of sufficiently large spectroscopic differences between polymorphs, quantification of the polymorph mixture can be performed accurately. As it was mentioned before, the characteristic absorption band of Form 2 at 1153 cm^{-1} was used for quantification. Figure 3 magnifies the absorbance band at 1153 cm^{-1} . To prevent the effect of size distribution of particles, it is best to use the ratio of the characteristic peak and a reference peak (inert peak) that is common to both polymorphs. For BUS-HCl, peaks at 1153 and 1193 cm^{-1} were chosen as characteristic and reference peak, respectively. The calibration plot, shown in Fig. 4, shows good linearity over the entire concentration range with a high correlation coefficient ($R^2 = 0.9806$). Figure 4 shows the calibration results for the mixture of two polymorphs as well as the linear equation.

Another approach for the quantitative analysis of a polymorphic mixture using the entire FTIR spectrum is the chemometric method. Chemometrics uses multivariate data analysis and mathematical tools to extract information from

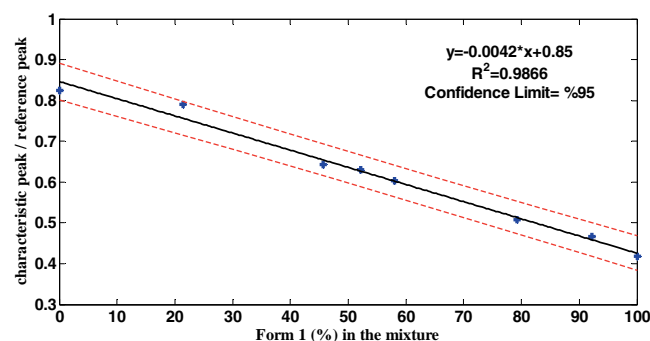


Fig. 4. The calibration curve for powder mixture of two polymorphs.

Table II. Comparison between Actual Value and Predicted Values with Two Chemometric Methods

Actual value (%)	Method	Predicted value								
		Combination 1, no. of factors			Combination 2, no. of factors			Combination 3, no. of factors		
		3	5	8	3	5	8	3	5	8
57.977	PCR	60.656	56.924	56.924	60.463	59.178	59.178	58.403	58.402	58.402
	PLS	N/A	55.306	55.306	60.213	59.178	59.178	58.402	58.402	58.402

the entire spectra. For the concentration matrix, different combinations of peaks (combinations 1 to 3) at 1118, 1134, 1153, and 1193 cm^{-1} were used. Peaks at 1153 and 1193 cm^{-1} are the characteristic peaks of Form 2 and the reference peaks used in the previous method. Combination 1 uses all four peaks listed above. Combination 2 utilizes the first and last two peaks. Combination 3 uses the characteristic and reference peaks. PCR and PLS methods were implemented on these data. The two methods were compared with a different combination of peaks and number of factors in each case. The factors set were the eigenvectors and eigenvalues that span the data in the concentration matrix.

Table II shows the results of several calculations with a different number of factors and concentration matrixes for one point in the mixture of two polymorphs. A key step in developing PCR and PLS calibrations is choosing the abstract factors (rank) between those factors that are analytically useful and those factors that are only model noise. Increasing the number of factors (optimal point) increases the amount of calculations. For example, in the PCR method with combination 1 of peaks, the results with five and eight factors are similar. In addition, the number of peaks is very important. If five factors are selected, predicted values from two peaks will be closer to the actual value rather than from four peaks. The reason for this is that the data from different peaks are cross-correlated and they cannot add more information to the concentration matrix, while increasing the error. The PCR and PLS methods have similar results for different combinations of peaks and factors. The PCR method has a linear equation for the calibration curve given by:

$$C = \sum_1^i \gamma_i A_i + \gamma_c \quad (1)$$

where C is the concentration, γ_i are constants corresponding to each peak, A_i are the maximum of each peak, and γ_c is

a constant. Table III shows different constants for the combinations of peaks. Figure 5 shows the actual vs. predicted values for two methods. The number of factors is five and concentration matrix includes two peaks (combination 3). The R^2 value for two methods confirms good prediction of the concentration values.

X-Ray Powder Diffraction

Each crystal form produces a diffraction pattern that can be used as a fingerprint for that form and thus can be used to screen polymorphs during drug discovery, formulation development, and manufacturing.

Figure 6 shows the XRPD spectra for two polymorphs of BUS-HCl. Similar XRPD diffraction patterns exist for the two polymorphs at 2θ angle positions 13.0°, 13.9°, 14.9°, 15.3°, 16.3°, 17.0°, 18.5°, 19.8°, 20.8°, 22.4°, 23.0°, 24.2°, 25.2°, 25.6°, and 26.6° with $\pm 0.2^\circ$ intervals. Form 1, however, has specific peaks at the following 2θ angles: 6.7°, 8.5°, 12.6°, 17.6°, 28.2°, 33.6°, and 44.8°. The unique 2θ angles for Form 2 are 7.4°, 10.0°, 18.9°, 20.0°, 21.7°, 29.3°, and 30.3°. These angles and their relative intensities can be used for polymorphic identity of the solid forms and for the quantitative determination of phase compositions. Good correlations between sample composition and scattering intensities were obtained for the two polymorphs. To reduce the effect of crystal size distribution on XRPD results, the samples were ground. Spinning or rocking the sample during data acquisition or combination of these methods can also be done. No polymorphic transformation was observed due to grinding of the samples.

Laser Raman Spectroscopy

Raman spectroscopy provides information about molecular vibrations that can be used for sample identifica-

Table III. PCR Constants for Different Combinations of Peaks for Five Factors

Combination	γ_i				γ_c
	1118 cm^{-1}	1134 cm^{-1}	1153 cm^{-1}	1193 cm^{-1}	
1	16.5572	-49.4008	-21.0728	38.5247	0.9773
2	2.5553	-	-20.0787	5.5526	0.8054
3	-	-	-22.5509	12.0541	0.7708

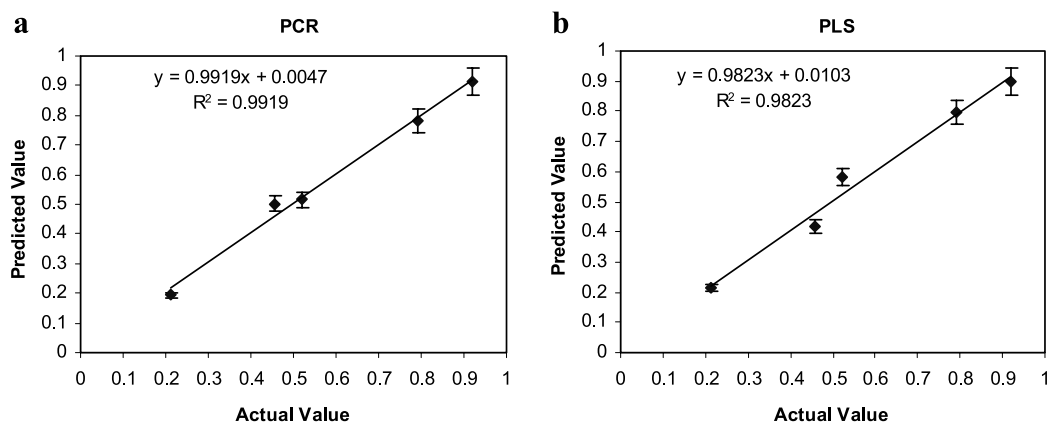


Fig. 5. Plot of predicted vs. actual percentages of Form 1 in Form 2.

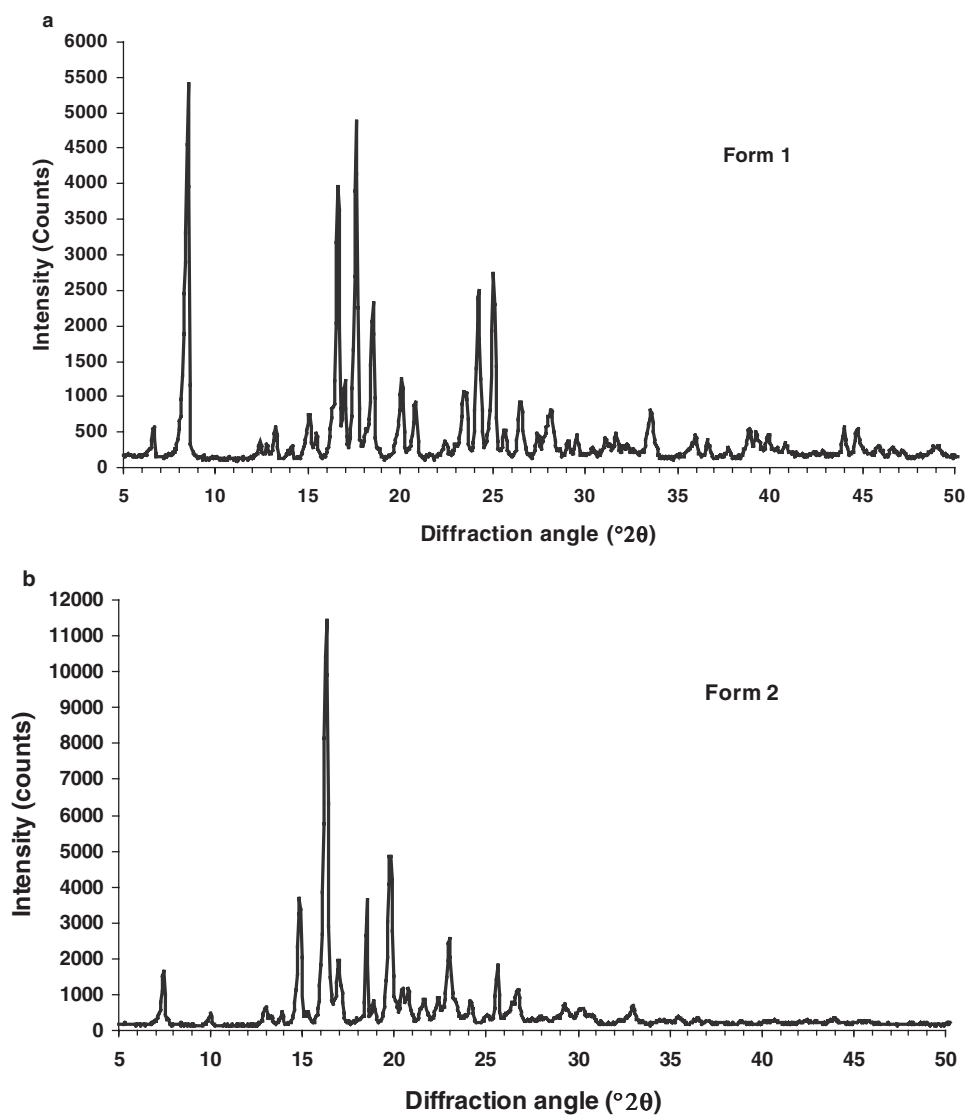


Fig. 6. XRPD patterns of BUS-HCl polymorphs: (a) Form 1 and (b) Form 2.

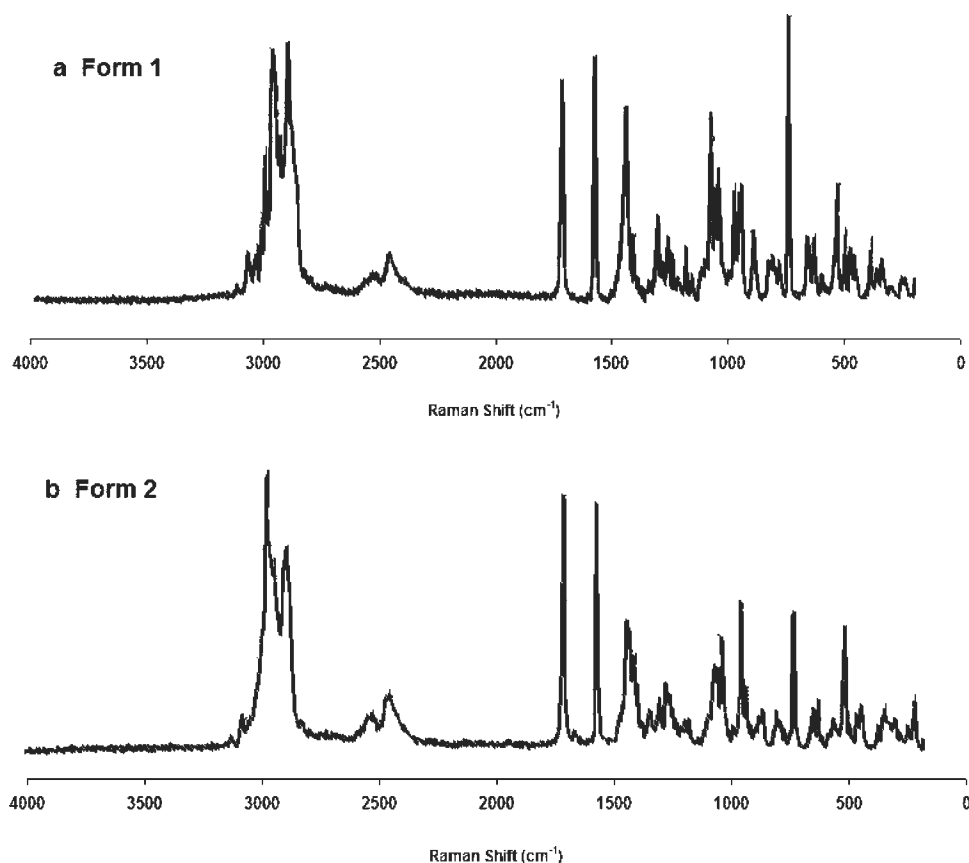


Fig. 7. Raman patterns of BUS-HCl polymorphs.

tion and quantitative analysis. The Raman effect is based on the inelastic scattering of laser light by molecules or crystals (7). For two polymorphs of BUS-HCl, the Raman method gave vibrational spectra of the samples in the range 200–4000 cm^{-1} . These spectra can be used for structural analysis, identification of crystal forms, and quantification assays. The Raman method did not require much sample preparation, and the relative intensities in the spectra were barely affected by sampling parameters. These qualify this technique for accurate quantitative analysis of solid components or polymorphs in drug formulations. Figure 7 shows the Raman spectra for two polymorphs of BUS-HCl. From comparison between the two spectra, unique shifts for each polymorph and common peaks for them can be identified. Table IV presents Raman peak information for the two forms.

CONCLUSIONS

Polymorphic forms of BUS-HCl were studied in detail in this work. Forms 1 and 2 of BUS-HCl can be distinguished by thermal analysis and crystallographic and spectroscopic methods because of differences in their melting points and unique vibrational and XRPD peaks. The samples of both forms were pure and TGA did not show any mass losses. DSC analysis demonstrated that the two polymorphs are enantiotropically related and heat of fusion rule confirmed that finding. The two polymorphs have conformational differences. Unique characteristic peaks in the FTIR spectra of the two forms were successfully utilized for the quantification and qualification of the powder mixtures. By using the ratio between two peaks of FTIR and chemometrics methods, the composition of each polymorph

Table IV. Raman Unique Peaks of BUS-HCl Polymorphs

	Raman shift (ppm)															
	328	460	522	560	590	610	790	840	970	985	1070	1420	2940	3000	3005	3030
Form 1		×		×			×		×		×		×	×	×	×
Form 2	×		×		×	×		×		×		×				

in a solid mixture can be determined. The XRPD and Raman spectroscopy methods show the difference between the two polymorphs.

ACKNOWLEDGMENT

The authors thank Apotex PharmaChem Inc., Brantford, Ontario, Canada, for providing buspirone free base samples.

REFERENCES

1. A. S. Raw, M. S. Faurness, D. S. Gill, R. C. Adams, F. O. Holcombe, and L. X. Yu. Regulatory considerations of pharmaceutical solid polymorphism in abbreviated new drug applications (ANDAs). *Adv. Drug Delivery Rev.* **56**:397–414 (2004).
2. R. J. Behme T. T. Kensler, and D. G. Mikolasek. U.S. Patent 4,810,789, 1989.
3. Z. Chilmonczyk, J. Cybulski, A. Szelejewska, and A. Les. NMR studies of buspirone analogues. *J. Mol. Struct.* **358**:195–207 (1996).
4. D. S. Aldrich and M. A. Smith. *Pharmaceutical Applications of Infrared Spectroscopy*, Marcel Dekker, Inc., New York, 1995.
5. A. Burger and R. Ramberger. *Mikrochim. Acta* **2**:259 (1979).
6. A. Burger and R. Ramberger. *Mikrochim. Acta* **2**:273 (1979).
7. T. Vankeirsblick, A. Vercauteren, and W. Baeyens. Applications of Raman spectroscopy in pharmaceutical analysis. *J. Pharm. Sci.* **89**:1342–1353 (2002).
8. H. G. Brittain (ed). *Polymorphism in Pharmaceutical Solids*, Marcel Dekker, New York, 1999.
9. M. Mirmehrabi, S. Rohani, K. S. K. Murthy, and B. Radatus. Solubility, dissolution rate and phase transition studies of ranitidine hydrochloride tautomeric forms. *Int. J. Pharm.* **282**:73–85 (2004).